

Location of the Potts-critical end point in the frustrated Ising model on the square lattice

Ansgar Kalz^{1,*} and Andreas Honecker^{1,2}

¹*Institut für Theoretische Physik, Georg-August-Universität Göttingen, 37077 Göttingen, Germany*

²*Fakultät für Mathematik und Informatik, Georg-August-Universität Göttingen, 37073 Göttingen, Germany*

(Dated: September 7, 2012)

We report on Monte-Carlo simulations for the two-dimensional frustrated J_1 - J_2 Ising model on the square lattice. Recent analysis has shown that for the phase transition from the paramagnetic state to the antiferromagnetic collinear state different phase-transition scenarios apply depending on the value of the frustration J_2/J_1 . In particular a region with critical Ashkin-Teller-like behavior, i.e., a second-order-phase transition with varying critical exponents, and a non-critical region with first-order indications were verified. However, the exact transition point $[J_2/J_1]_C$ between both scenarios was under debate. In this paper we present Monte-Carlo data which strengthens the conclusion of Jin *et al.* [PRL **108**, 045702 (2012)] that the transition point is at a value of $J_2/J_1 \approx 0.67$ and that double-peak structures in the energy histograms for larger values of J_2/J_1 are unstable in a scaling analysis.

PACS numbers: 64.60.De, 75.10.Hk, 05.70.Jk, 75.40.Mg

I. INTRODUCTION

The introduction of competing interactions in the classical two-dimensional J_1 - J_2 Ising model is accompanied by the appearance of new ground states and critical points at which the ground state shows a large degeneracy. Additionally the frustration can also affect the critical behavior of the model. In particular the emergence of varying critical exponents for the transition from a high-temperature paramagnetic phase to a collinear phase was observed numerically.^{1,2}

However, a scenario of a continuous phase transition with varying exponents was in question after mean-field calculations by Lopéz *et al.*^{3,4} gave evidence for a first-order transition in a certain regime of the frustration. The first-order scenario was strengthened by Monte-Carlo simulations which mainly focused on the evaluation of energy histograms at the critical temperature.^{5,6}

Recently we presented in Ref. 7 a full analysis for the phase transition using conformal field theory and extensive Monte-Carlo simulations. The focus was on the derivation of the underlying field theory starting at the point of two decoupled Ising models at $J_1 = 0$ which is represented by a $c = 1$ field theory. By including the nearest-neighbor coupling J_1 perturbatively we arrived at an Ashkin-Teller field theory which has a central charge of $c = 1$ and is known to exhibit varying critical exponents.⁸ Moreover, the Potts-critical end point of this theory allows for the onset of a non-critical phase transition^{9,10} and could thereby explain the two different scenarios observed in the frustrated Ising model. The energy histograms showed two-peaked structures in the intermediate regime $J_1/2 < J_2 \lesssim J_1$. This led to the conclusion that the position of the critical end point was at $J_1 \approx J_2$. Jin *et al.*¹¹ agree with the general picture of two different transition scenarios and an underlying Ashkin-Teller field theory but argue that the first-order behavior

is only valid up to $J_2 \lesssim 0.67 J_1$. Using mainly arguments about the universality of the Binder cumulants they show the equivalence of the point $J_2 \approx 0.67 J_1$ in the frustrated Ising model and the 4-state Potts model¹² which marks the critical end point of the Ashkin-Teller field theory.⁸⁻¹⁰

While the finite-size dependence of the histogram shape was analyzed for small parameters $J_2 = 0.6 J_1$ and $0.65 J_1$ ^{5,6} such an analysis was not performed for $J_2 \geq 0.7 J_1$ due to the increasing length scales needed to exhibit the double-peak structure in the first place. Thus, the onset of doubly-peaked features in the histograms was interpreted as signal for a first-order transition. In this work we present a finite-size analysis for the energy histograms on a larger scale and observe the vanishing of first-order signals for $J_2 \gtrsim 0.67 J_1$ in agreement with the conclusion of Jin *et al.*¹¹ that the first-order scenario ends at $J_2 \approx 0.67 J_1$. Furthermore we analyze the trend of the critical exponents in the intermediate regime $0.67 J_1 < J_2 \leq 1.2 J_1$ to prove the convergence of the Ashkin-Teller model and its exponents to the Potts-critical end point.

After a short introduction to the model in Sec. II we present new Monte-Carlo results for histograms and critical exponents in Sec. III; in particular the scaling analysis will be presented exemplary at the point $J_2 = 0.8 J_1$. We summarize our results in the concluding Sec. IV.

II. MODEL

The frustrated Ising model is described by the classical Hamiltonian

$$H_{\text{Ising}} = J_1 \sum_{\text{NN}} S_i S_j + J_2 \sum_{\text{NNN}} S_i S_j \quad (1)$$

which sums over all antiferromagnetic ($J_1, J_2 > 0$) nearest-neighbor (NN) and next-nearest-neighbor (NNN) interactions of spin variables $S_i = \pm 1$ on a square lattice.

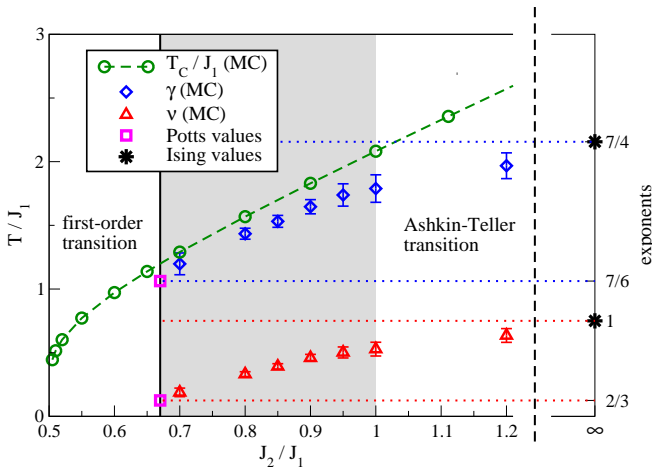


FIG. 1. (Color online) Phase diagram for the frustrated Ising model for $J_2 > J_1/2$. Two different regions are identified where the phase transitions show different behavior. In particular the shaded area in the middle is discussed in this work by means of histograms and critical exponents (ν red triangles and γ blue diamonds). Data for the critical temperatures (green circles) are from Ref. 7.

Ground-state configurations are given by a two-fold degenerate Néel state for $J_2 < J_1/2$ and a four-fold degenerate collinear state for $J_2 > J_1/2$. At the critical point $J_2 = J_1/2$ the transition temperature is suppressed to zero and a ground-state manifold with a degeneracy of linear order is present.⁵ The phase transition to the Néel state belongs to the $2D$ -Ising universality class and will not be discussed any further. However, for $J_2 > J_1/2$ two different phase-transition scenarios apply for small and large values of frustration J_2/J_1 : Ashkin-Teller like critical behavior with varying critical exponents for $J_2/J_1 \nearrow \infty$ and first-order non-critical phase transitions for $J_2/J_1 \searrow 0.5$.^{7,11} In Fig. 1 the critical temperatures are shown as green circles; the exact transition point between both regimes will be discussed in the following section and the area in question is marked in gray.

III. MONTE-CARLO RESULTS

For the following numerical analysis we used a single-spin Metropolis update¹³ with additional temperature exchange Monte-Carlo steps^{14–16} as it was also used in earlier works on the frustrated Ising model.^{5–7}

To investigate the nature of the phase transition the first focus was on the computation of energy distributions. In Ref. 7 we presented a histogram at $J_2 = 0.8 J_1$ for a lattice of linear size $L = 1000$ with a double-peak feature. This was interpreted as evidence for a first-order transition. For this work we computed systems with $L = 1000, 1200, 1500, 2000$ and present in Fig. 2 histograms at the size-dependent critical temperature.

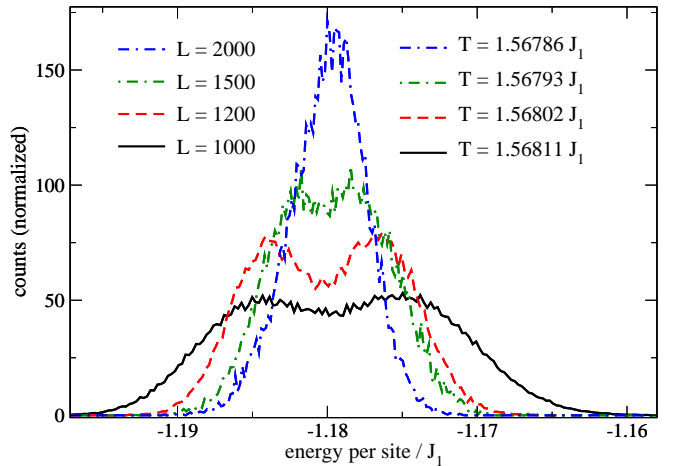


FIG. 2. (Color online) Histograms for different lattice sizes recorded for critical (size dependent) temperatures at $J_2 = 0.8 J_1$. After the emergence of a double peak at intermediate system sizes $L = 1000, 1200$ the vanishing of this first-order signature is observed for even larger systems ($L = 1500, 2000$).

Surprisingly an extinction of the doubly-peaked shape is observed for $L > 1200$. The distance between the two peaks decreases and vanishes completely when the linear system size is doubled. Thus, the scenario of a first-order transition is no longer valid for the intermediate value of $J_2 = 0.8 J_1$ and further analysis of the critical behavior is necessary.

In the light of the recent work by Jin *et al.*¹¹ we checked the development of critical exponents for varying frustration $J_2/J_1 \searrow 0.67$ by analyzing our Monte-Carlo data for system sizes from $N = 50 \times 50$ to $N = 500 \times 500$. A detailed investigation of correlation functions and the corresponding exponent η would not be meaningful since $\eta = 1/4$ is expected to be constant in the Ashkin-Teller model.¹⁰ By applying the scaling relation $\gamma/\nu = 2 - \eta$ the ratio of $\gamma/\nu = 7/4$ is also fixed.^{10,11} However, the exponents γ and ν can be extracted separately. In particular the Binder cumulants^{17,18} U_B and the susceptibility χ

$$U_B = 1 - \frac{\langle m^4 \rangle}{3\langle m^2 \rangle^2} \quad \wedge \quad \chi = \frac{\langle m^2 \rangle}{T \cdot L^2} \quad (2)$$

for the collinear phase have been computed for this purpose. The order parameter is defined as

$$m = m_x + m_y, \quad m_{x,y} = \frac{1}{N} \sum_i (-1)^{i_{x,y}} S_i \quad (3)$$

and satisfies $\langle m \rangle = 0$ for all temperatures in finite systems. The results were double-checked for some parameters with a slightly different definition of the order parameter $m^2 = m_x^2 + m_y^2$ which was used in Ref. 11. In the scaling analysis for critical temperatures and exponents we did not notice any differences.

The critical exponent ν of the correlation length ξ is calculated from the scaling of derivatives for Binder

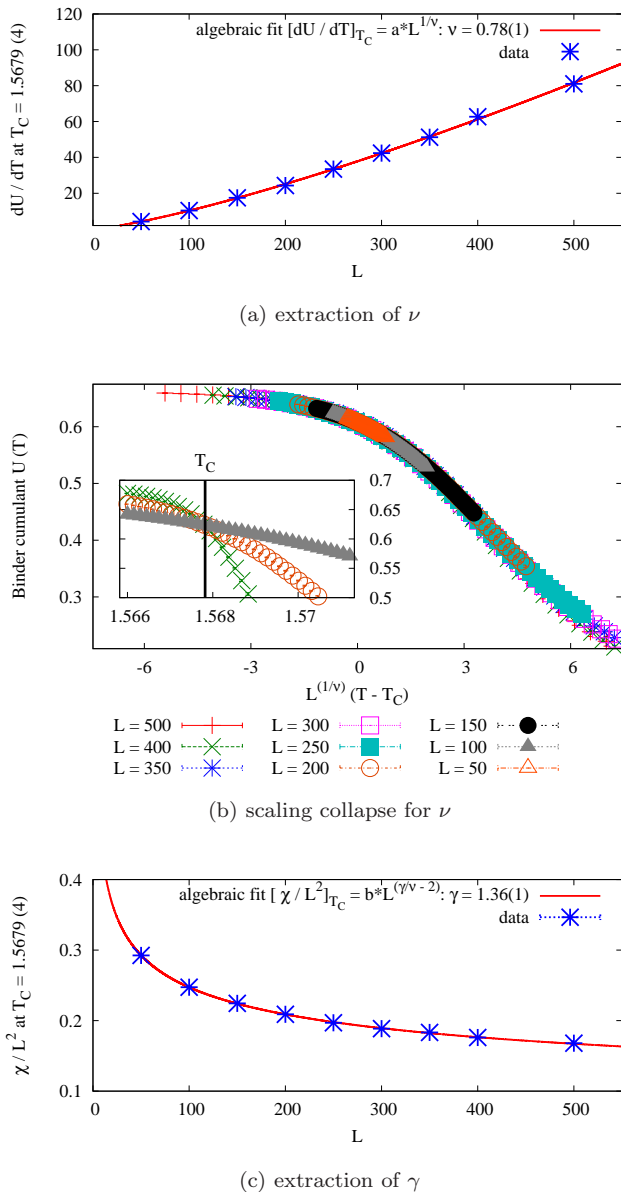


FIG. 3. (Color online) Computation of critical exponents ν and γ from the Binder cumulants and susceptibility of the magnetic order parameter at $J_2 = 0.8 J_1$. Figs. (a) and (c) show size-dependent values of the derivative $[dU/dT]_{T_C}$ and susceptibility $[\chi/L^2]_{T_C}$ and algebraic fits that yield $\nu = 0.78(1)$ and $\gamma = 1.36(1)$. In the middle panel (b) additionally a scaling collapse of the Binder cumulant is shown for given T_C and ν ; three original Binder cumulants are shown in the inset.

cumulants of different system sizes at the transition temperature:^{2,5}

$$dU_B/dT|_{T_C} = a \cdot L^{1/\nu}. \quad (4)$$

Hereby we neglect scaling corrections which have only small influence on the resulting exponent, i.e., the deviation is smaller than the fitting error. Exemplary the scaling analysis is shown for $J_2 = 0.8 J_1$ in Fig. 3(a): at

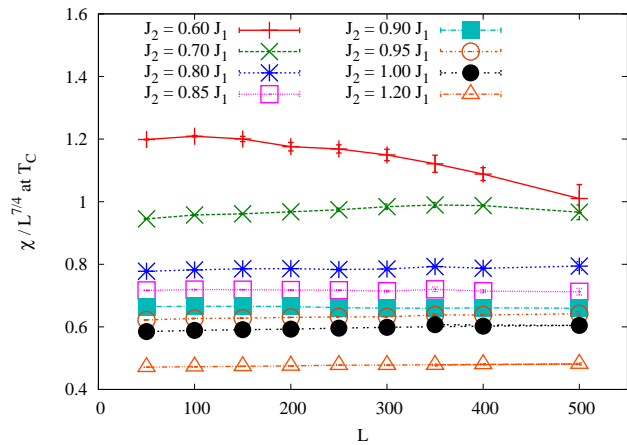


FIG. 4. (Color online) Flowgrams for the susceptibility χ at the transition temperature T_C for several ratios J_2/J_1 . Only for $J_2 \gtrsim 0.7 J_1$ the scaling is nearly constant in $L^{-7/4}$ and Ashkin-Teller-like behavior is obtained.

the critical temperature $T_C = 1.5679(4) J_1$ a critical exponent $\nu = 0.78(1)$ is extracted. The same values are used in a finite-size-scaling collapse^{2,19,20} of the Binder cumulants vs. $L^{1/\nu}(T - T_C)$ in Fig. 3(b), and the good agreement in a wide temperature and lattice-size regime verifies the assumption of criticality in general and confirms the extracted values in particular. The same procedure was performed for several ratios of $J_2/J_1 > 0.67$ and all values of ν are shown in Fig. 1 as red triangles. It is clearly observable that the exponents vary monotonically from the Ising value $\nu_{\text{Ising}} = 1$ for $J_1 = 0$ (right-hand side) towards the 4-state Potts value¹² $\nu_{\text{Potts}} = 2/3$ for $J_2/J_1 \searrow 0.67$ (straight black vertical line). A comparison with earlier works is ambiguous: Our values for ν and $J_2 \geq 0.7 J_1$ are in good agreement with the data presented in Ref. 21 albeit our values have smaller errors. However, more recent analyses at the point $J_2 = J_1$ yield a value of roughly $\nu = 0.84(1)$ ²²⁻²⁴ at $T_C = 2.082(1) J_1$ whereas our analysis yields a value of $\nu = 0.88(2)$ for a critical temperature $T_C = 2.0819(4) J_1$. This discrepancy shows the importance of the additional scaling-collapse analysis which helps to refine the critical temperature and exponent.

A similar scaling analysis is performed for the susceptibility and is also shown exemplary at $J_2 = 0.8 J_1$ in Fig. 3(c). However, the critical exponent γ also depends on the previously extracted ν and is obtained without scaling corrections via:

$$\chi|_{T_C} = b \cdot L^{\gamma/\nu}. \quad (5)$$

The development of $\gamma(J_2/J_1)$ is illustrated by the blue diamonds in Fig. 1. The limits are given by $\gamma_{\text{Ising}} = 7/4$ and $\gamma_{\text{Potts}} = 7/6$.¹² Along the line of phase transitions the ratio of γ and ν is roughly constant at $7/4$ which is valid for both the Ising model and the Ashkin-Teller model including the Potts-critical end point. This fact is also observable from the flowgram presented in Fig. 4:

We present the flowgram of the susceptibility for different parameters J_2/J_1 in addition to the scaling analysis. According to Refs. 19 and 25 the behavior of the flow of some observable connected to the phase transition should change significantly if the type of this transition is altered. Such an alteration is visible in Fig. 4 for the flow at $J_2/J_1 = 0.6$ which is not constant in the chosen scaling over $L^{-7/4}$. For all other parameters, i.e., $J_2/J_1 \geq 0.7$ the flow of the susceptibility shows only small deviation from a constant scaling which fits into the picture of the Ashkin-Teller critical behavior.

IV. DISCUSSION

We presented new Monte-Carlo data on the paramagnetic-collinear phase transition in the frustrated Ising model. Our data are in agreement with the recent findings of Jin *et al.*¹¹ and provide further support for the Ashkin-Teller nature of this phase transition in a specified parameter region. In particular we analyzed the evolution of the critical exponents ν and γ from their Ising values [at $J_2/J_1 \nearrow \infty$] to the 4-state-Potts values [at $J_2/J_1 \approx 0.67$]. Thus, the critical frustration parameter of $[J_2/J_1]_C \approx 0.67$ proposed by Jin *et al.* is

confirmed by our analysis. A comparison of the absolute values of ν with estimates given by Landau and Binder²¹ shows good agreement and smaller errors for our data. However, at the present level of accuracy the values deviate from recent findings of several other groups.²²⁻²⁴ We also presented a finite-size analysis for the energy distribution at $J_2 = 0.8 J_1$ and showed that first-order signals in the histograms vanish for linear system sizes $L > 1200$ and thereby the scenario of a critical phase transition is strengthened also by the absence of a latent heat.

ACKNOWLEDGMENTS

We thank the Deutsche Forschungsgemeinschaft for financial support via the Collaborative Research Centre SFB 602 (TP A18). Furthermore, the Monte-Carlo simulations were performed on the parallel clusters of the Gesellschaft für wissenschaftliche Datenverarbeitung Göttingen (GWDG) and the North-German Supercomputing Alliance (HLRN) and we thank them for technical support. We acknowledge fruitful discussions with Anders Sandvik and Arnab Sen (authors of Ref. 11) and Pierre Pujol from the University of Toulouse.

* kalz@theorie.physik.uni-goettingen.de

¹ K. Binder and D. P. Landau, Phys. Rev. B **21**, 1941 (1980).

² D. P. Landau and K. Binder, *Monte Carlo Simulations in Statistical Physics*, 1st ed. (Cambridge University Press, 2000).

³ J. Morán-López, F. Aguilera-Granja, and J. Sanchez, Phys. Rev. B **48**, 3519 (1993).

⁴ J. Morán-López, F. Aguilera-Granja, and J. Sanchez, J. Phys.: Cond. Matt. **6**, 9759 (1994).

⁵ A. Kalz, A. Honecker, S. Fuchs, and T. Pruschke, Eur. Phys. J. B **65**, 533 (2008).

⁶ A. Kalz, A. Honecker, S. Fuchs, and T. Pruschke, J. Phys.: Conf. Ser. **145**, 012051 (2009).

⁷ A. Kalz, A. Honecker, and M. Moliner, Phys. Rev. B **84**, 174407 (2011).

⁸ P. Ginsparg, in *Fields, strings and critical phenomena*, edited by E. Brézin and J. Zinn Justin (Session XLIX, Les Houches, 1988).

⁹ R. Ditzian, J. Banavar, G. Grest, and L. Kadanoff, Phys. Rev. B **22**, 2542 (1980).

¹⁰ R. J. Baxter, *Exactly solved models in statistical mechanics* (Academic Press, London, 1982).

¹¹ S. Jin, A. Sen, and A. Sandvik, Phys. Rev. Lett. **108**, 045702 (2012).

¹² F. Y. Wu, Rev. Mod. Phys. **54**, 235 (1982).

¹³ N. Metropolis, A. W. Rosenbluth, M. N. Rosenbluth, A. H. Teller, and E. Teller, J. Chem. Phys. **21**, 1087 (1953).

¹⁴ K. Hukushima and K. Nemoto, J. Phys. Soc. Jp. **65**, 1604 (1996).

¹⁵ U. H. Hansmann, Chem. Phys. Lett. **281**, 140 (1997).

¹⁶ H. G. Katzgraber, S. Trebst, D. A. Huse, and M. Troyer, J. Stat. Mech.: Theory and Experiment, P03018 (2006).

¹⁷ K. Binder, Phys. Rev. Lett. **47**, 693 (1981).

¹⁸ K. Binder, Z. Phys. B Cond. Matt. **43**, 119 (1981).

¹⁹ A. Kuklov, M. Matsumoto, N. Prokof'ev, B. Svistunov, and M. Troyer, Phys. Rev. Lett. **101**, 050405 (2008).

²⁰ D. Charrier, F. Alet, and P. Pujol, Phys. Rev. Lett. **101**, 167205 (2008).

²¹ D. P. Landau and K. Binder, Phys. Rev. B **31**, 5946 (1985).

²² A. Malakis, P. Kalozoumis, and N. Tyraskis, Eur. Phys. J. B **50**, 63 (2006).

²³ J. Yin and D. P. Landau, Phys. Rev. E **80**, 051117 (2009).

²⁴ A. K. Murtazaev, M. K. Ramazanov, and M. K. Badiev, Low Temp. Phys. **37**, 1001 (2011).

²⁵ A. Kuklov, N. Prokof'ev, B. Svistunov, and M. Troyer, Ann. Phys. **321**, 1602 (2006).